Journal of Alloys and Compounds, 202 (1993) 289–294
JALCOM 849

$K_8In_{10}Hg$: a Zintl phase with isolated $In_{10}Hg$ clusters

Slavi C. Sevov, Jerome E. Ostenson and John D. Corbett*
Ames Laboratory-DOE and Department of Chemistry, Iowa State University, Ames, IA 50011 (USA)

(Received April 2, 1993, in final form June 8, 1993)

Abstract

The title compound results from the substitution of one mercury atom for indium in the known metallic K_8In_{11} [$8K^+ + In_{11}^{7-} + e^-$]. It contains the same isolated eleven-atom clusters as before, pentacapped trigonal prisms compressed along the three-fold axis, but with mercury disordered over the trigonal prismatic sites ($P6_3/m$, $Z=2$, $a=9.9812(4)$ Å, $c=16.851(1)$ Å, $R/R_w=2.4/2.8\%$). The cluster $In_{10}Hg^{8-}$ is likewise hypoelectronic and requires the $2n-4=18$ skeletal bonding electrons available for this stoichiometry. The close-packed layers of clusters are again separated by double layers of potassium, but these follow an h.c.p. order rather than the c.c.p. arrangement found in K_8In_{11}. The phase is diamagnetic ($\sim -3.5\times10^{-4}$ emu mol^{-1}), in contrast to the Pauli-like behavior of K_8In_{11}, but it too exhibits a conductivity characteristic of a poor metal or a semimetal, $\rho_{295}\sim270$ $\mu\Omega^{-1}$ cm^{-1} with a coefficient of $+0.48\%$ deg^{-1}.

1. Introduction

The supposedly simple alkali-metal–indium systems are proving to be rich in novel cluster chemistry, revealing a considerable disposition toward homoatomic bonding in closed-shell, valence-precise situations [1–6]. Most of the indium products appear to be very distinctive relative to those formed by its congener gallium [7], especially in the formation of isolated and centered clusters. The first example was the remarkable K_8In_{11} in which close-packed layers of isolated pentacapped trigonal prisms ($\sim D_{3h}$) both contain potassium atoms and are separated by double potassium layers [1]. A formal In_{11}^{8-} anion with an odd number of electrons would be improbable, and, in fact, molecular orbital (MO) calculations as well as magnetic and conductivity measurements show that the metallic compound should be formulated in terms of one delocalized electron per hypoelectronic ($2n-4$) cluster In_{11}^{7-}. Both axial capping and compression of a conventional tricapped trigonal prism account for the unusual electronic configuration, well below the classical $2n+2$ "floor" predicted by Wade's rules for normal closo deltahedra [8].

Two other types of isolated clusters have been found in addition to numerous phases containing interconnected clusters, some of novel design [2, 3, 6]. The first is the zinc-centered $In_{10}Zn^{8-}$ as the potassium salt. The anion is based on a bicapped antiprism (D_{4d}) in which a cluster expansion and the zinc interstitial reduce the classical 12− charge to 8− [4]. Another type of cluster found in $K_{10}In_{10}M$, M=Ni, Pd, Pt, is best described as M-centered, tetracapped trigonal prisms of approximately C_{3v} symmetry [6].

The novelty of a closed-shell cluster In_{11}^{7-} in a solid that is also metallic by virtue of an extra electron, viz. $(K^+)_8In_{11}^{7-}e^-$, has prompted us to search for derivatives in which the odd electron might instead be bound. One obvious way to accomplish this would be by substitution of a zinc family element into the cluster since these are one electron poorer. Zinc itself gives instead the centered $In_{10}Zn^{8-}$ (above), cadmium produces a complex network structure [6], but mercury gives us the desired result $In_{10}Hg^{8-}$ in the potassium salt.

2. Experimental section

The reaction techniques in welded tantalum tubing have been described before [2, 3]. All materials were handled in an N_2-filled glovebox. A mixture of the elements (K–J.T. Baker, lump under oil, 98+%; In–Cerac, 99.999%; Hg–Fisher, instrument grade) in proportions appropriate to produce $K_8In_{10}Hg$ was allowed to react at 600 °C for 2 days, quenched to room temperature, and then annealed at 400 °C for 10 days. The product was dark gray, very brittle and had a metallic lustre. The compound in air changes to a bubbling liquid in less than a minute. A few crystallites were selected, sealed in capillaries, and checked by

*Author to whom correspondence should be addressed.

0925-8388/93/$6.00

TABLE 1. Data collection and refinement parameters for $K_8In_{10}Hg$

Crystal size, mm	0.05×0.12×0.20
Lattices parameters[a]	
a, Å	9.9812(4)
c, Å	16.851(1)
V, Å^3	1453.8(1)
Space group, Z	$P6_3/m$, (No. 176), 2
Diffractometer, temperature (°)	CAD4, 21
Radiation, 2θ(max)	Mo Kα, graphite monochromated; 50°
Octants measured	$\pm h$, k, l
Scan method	$\omega-2\theta$
No. of reflections measured	2804
Obs. ($I>3.00\ \sigma_I$)	1897
Indep. obs.	611
Abs. coeff. (Mo Kα), cm^{-1}	140.5
Transmittance factor range	0.5002–1.0
R(ave), (all data) %	4.7
No. variables	34
Residual R; R_w[b](%)	2.4; 2.8
Maximum shift/σ in final cycle	0.00
Largest peaks in final ΔF, e/Å^3	+1.06 (1.0 Å from In3), −0.72
Sec. ext. coeff. (10^{-8})	8 (2)

[a]Guinier data with Si internal standard, $\lambda=1.540\ 562$ Å.
[b]$R=\Sigma||F_o|-|F_c||/\Sigma|F_o|$; $R_w=[\Sigma w(|F_o|-|F_c|)^2/\Sigma w(F_o)^2]^{1/2}$; $w=\sigma_F^{-2}$.

oscillation and Weissenberg film techniques for singularity and an eventual space group assignment.

A plate-like single crystal (0.05×0.12×0.20 mm) was chosen and mounted on a CAD4 single crystal diffractometer. (Some details of the data collection and refinement are listed in Table 1). The 25 reflections from a random search were indexed with a hexagonal unit cell of the same dimensions as already estimated from the Weissenberg photographs. Two octants of data were collected at room temperature with monochromated MoKα radiation ($2\theta_{max}=50°$). The data were consistent with three possible space groups, $P6_3$, $P6_3/m$ and $P6_322$, after corrections for Lorentz and polarization effects as well as for absorption with the aid of the average of two ψ-scans collected at different θ values. Wilson plot statistics showed a centrosymmetric type distribution, so $P6_3/m$ was chosen and was later shown to be correct.

Application of direct methods (SHELX-86 [9]) gave three positions with distances around each appropriate to In–In bonds. Subsequent least-squares refinement and difference Fourier synthesis with these revealed three additional positions that were assigned to potassium. A few least-squares cycles with anisotropic thermal parameters led to $R=3.6\%$ but a quite small B_{eq} for In3 compared with those for In1 and 2. Refinement of the occupancies of the indium atoms with all K atoms fixed showed 115% (18σ high) occupancy for the In3 site and comparable B_{eq} values for all three. The behavior suggested that a heavier atom, Hg in our case, was mixed with indium on the In3 position. Consequently, a mixture of indium and mercury was refined in this position with the constraint of 100% occupancy. This led to a drop of $R(F)$ to the final value, 2.4% ($R_w=2.8\%$). The occupancies of the other In sites did not deviate from unity by more than 2% (1.5σ) when the K atoms were kept fixed, and the K sites by more than 5% (4σ) when the In atoms were held fixed. The refined composition with only proportions at the In3 site varying was $K_8In_{9.97(3)}Hg_{1.03(3)}$ which agreed very well with the composition determined by EDX–$K_8In_{10.0(2)}Hg_{1.0}$. The largest peaks in the final difference Fourier map were 1.06 e Å^{-3} (1.0 Å from In3) and −0.72 e Å^{-3}. Note that the mercury-free K_8In_{11} occurs in a different space group, $R\bar{3}c$.

The powder pattern of the compound was obtained from a small portion of a powdered sample mounted between pieces of cellophane tape. An Enraf-Nonius Guinier camera, Cu Kα_1 radiation ($\lambda=1.540\ 562$ Å) and NBS (NIST) silicon as an internal standard were employed for this purpose. The least-squares refinement of measured 2θ values indexed on the basis of a calculated pattern gave the reported lattice dimensions.

The electrical resistivity of the phase was measured by an electrodeless "Q" method [10] over the temperature range 160–295 K with readings taken every 20°. The magnetization of the compound was measured at field of 3 Tesla over the range 6–295 K on a Quantum Design MPMS SQUID magnetometer. The containment procedures are described in more detail elsewhere [2].

3. Results and discussion

Atom parameters and important distances and angles for $K_8In_{10}Hg$ are listed in Tables 2 and 3, respectively.

TABLE 2. Positional and thermal parameters for $K_8In_{10}Hg$

Atom	Position	x	y	z	B_{eq}	Occupancy ($\neq 1$)
In1	6h	0.4638(1)	0.3457(1)	1/4	2.05(3)	
In2	4f	2/3	1/3	0.100 48(6)	2.07(3)	
In3	12i	0.368 22(6)	0.053 69(7)	0.156 90(4)	2.61(3)	0.828(5)
Hg	12i	(0.368 22)	(0.053 69)	(0.156 90)	(2.61)	0.172
K1	12i	0.6296(3)	0.0695(3)	0.4349(1)	3.42(9)	
K2	2a	0	0	1/4	3.6(2)	
K3	2c	1/3	2/3	1/4	4.0(2)	

Atom	U_{11}[a]	U_{22}	U_{33}	U_{12}	U_{13}	U_{23}
In1	0.0298(5)	0.0239(5)	0.0277(5)	0.0121(5)	0	0
In2	0.0283(4)	U_{11}	0.0221(6)	$U_{11}/2$	0	0
In3, Hg	0.0297(4)	0.0323(4)	0.0327(4)	0.0121(3)	−0.0032(3)	−0.0077(3)
K1	0.063(2)	0.042(1)	0.033(1)	0.032(1)	−0.000(1)	0.002(1)
K2	0.043(2)	U_{11}	0.049(4)	$U_{11}/2$	0	0
K3	0.048(2)	U_{11}	0.056(4)	$U_{11}/2$	0	0

[a] $T = \exp[-2\pi^2(U_{11}h^2a^{*2} + U_{22}k^2b^{*2} + U_{33}l^2c^{*2} + 2U_{12}hka^*b^* + 2U_{13}hla^*c^* + 2U_{23}klb^*c^*)]$.

TABLE 3. Important distances (Å) and intracluster angles (deg) in $K_8In_{10}Hg$[a]

In1		In3		K1		K2	
2 In1	3.618(2)	In1	3.0142(9)	In1[b]	3.580(2)	3 In1	4.1672(9)
2 In2	3.273(1)	In1	3.0317(9)	In2[b]	3.895(2)	6 In3	3.7798(6)
2 In3	3.0142(9)	In2	3.0420(7)	In2[c]	3.960(3)	6 K1	4.615(2)
2 In3	3.0317(9)	In3	3.138(1)	In3[d]	3.641(2)		
2 K1[b]	3.580(2)	In3[e]	5.005(1)	In3[b]	3.730(2)	K3	
K2	4.1672(9)	K1[d]	3.641(2)	In3[c]	3.744(2)	3 In1	4.0166(8)
K3	4.0166(8)	K1[b]	3.730(2)	In3[b]	3.868(2)	6 In1	4.0199(6)
		K1[c]	3.744(2)	2 K1	4.040(3)	6 K1	4.195(2)
In2		K1[b]	3.868(2)	K1	4.125(4)		
3 In1	3.273(1)	K2	3.7798(6)	2 K1[f]	4.865(2)		
3 In3	3.0420(7)	K3	4.0199(6)	K2	4.615(2)		
3 K1[b]	3.895(2)			K3	4.195(2)		
3 K1[c]	3.960(3)						

atom	atom	atom	angle
In2	In1	In2	100.68(3)
In2	In1	In3	57.70(1), 57.55(2)
In2	In1	In3	105.48(3), 105.08(3)
In3	In1	In3	62.73(3), 62.32(3)
In3	In1	In3	111.75(2)
In3	In1	In3	155.40(3)
In1	In2	In1	67.11(3)
In1	In2	In3	56.88(2), 57.24(2)
In1	In2	In3	111.45(4)
In3	In2	In3	110.70(2)
In1	In3	In1	73.51(3)
In1	In3	In2	65.42(2), 65.21(2)
In1	In3	In3	58.64(1), 58.84(1)
In2	In3	In3	108.21(2)

[a] $d(\text{K–In}) \leq 5.72$ Å; $d(\text{In–In}) \leq 5.76$ Å. All In3 sites contain 5/6 In, 1/6 Hg.
[b] Face-capping distances.
[c] Second K1 layer.
[d] Exo bond.
[e] Edge of the triangle in the trigonal prism.
[f] The only intralayer K–K distance within range.

Structure factor data (5 pages) are available from J.D.C.

A view of the $In_{10}Hg$ cluster is shown on Fig. 1. Open ellipsoids represent In1 and 2, the face and axial capping atoms, respectively, while the crossed members define the trigonal prism over which In3 and Hg are disordered in a 5:1 atomic ratio. There are two clusters per unit cell centered at 2*d* ($\bar{6}$) positions 2/3, 1/3, 1/4 and 1/3, 2/3, 3/4. The geometry of the cluster is effectively the same as In_{11} in K_8In_{11} although there are minor differences in the point group symmetries. The triangle of face-capping In1 atoms in $In_{10}Hg$ is rotated around the three-fold axis by 0.29° relative to the trigonal prism so that the In1 atoms are not exactly above the center of the rectangular faces, meaning that In1 has two different distances to In3(Hg)–3.032 (1) Å and 3.014 (1) Å. This reduces the symmetry from D_{3h} to C_{3h}. In the In_{11} cluster, the two triangles that define the trigonal prism are instead twisted by 3.1° with respect to each other, and the symmetry is again reduced, this time to D_3 [1].

The average In–In bond distances in the two clusters differ by only 0.006 Å. The distances from the mixed In3,Hg position to In1 and In3 are naturally slightly larger (3.023(av.) and 3.138 Å, respectively) than the corresponding values in K_8In_{11} (3.011(av.) and 3.097 Å), befitting the mercury substitution. The seemingly large thermal ellipsoid for the In3,Hg site also reflects this.

Figure 2 shows general views of the structures of K_8In_{11} (left) and of $K_8In_{10}Hg$ (right). The clusters in both structures lie in close-packed layers but the stacking

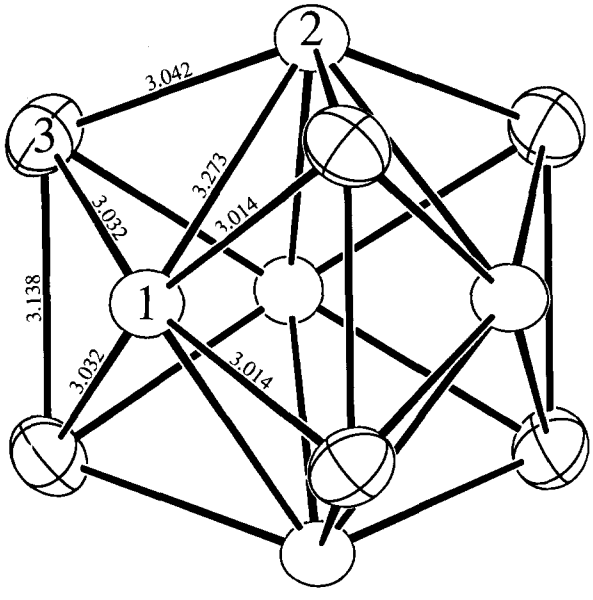

Fig. 1. The $In_{10}Hg$ cluster in $K_8In_{10}Hg$ with the three-fold axis vertical (94% probability ellipsoids). The trigonal prismatic atoms 3 are 5/6 In, 1/6 Hg while In1 and In2 cap all faces thereof. Distances in Ångstroms.

is different. In K_8In_{11} they follow a cubic (ABC) stacking and the cell is rhombohedral, while in $K_8In_{10}Hg$ the packing order and the space group are hexagonal (AB). Double layers of K1 atoms with very similar distances separate the layers of clusters in both structures. The other potassium atoms (K2 in K_8In_{11}, K2 and K3 in $K_8In_{10}Hg$) lie within the cluster layers. The quadrilateral (In3–In2–In3–In1) faces at both ends of the cluster are each capped by K1 atoms that are also neighbors of In2 and In2–In3 edges in other clusters through the double K1 layers. The triangular (In3–In1–In3) faces around the cluster waist are capped by six more potassium (K2 and K3 here), each of which is similarly bonded to two other clusters. The compounds can also be approximated as close packed layers of h.c.p. $K_6K_{6/3}In_{10}Hg$ or c.c.p. $K_6K_{6/3}In_{11}$ units. This specificity of alkali-metal bonding through edge-bridging or face-capping of indium cluster units seems quite general.

Since the structure of $K_8In_{10}Hg$ looks very much like a polymorph of the K_8In_{11}, additional work was done in order to establish that the compound is indeed a ternary phase. A reaction designed to produce the phase without mercury was run under exactly the same conditions as described in Section 2, but the product was only the known K_8In_{11}. The EDX results (experimental) and the change in space group also reassured us that a real substitution had occurred. The mercury compound has a 7.8 $Å^3$ larger formula volume, but reasonable comparative data for such an $Hg–In^+$ interchange cannot be found.

The location of the mercury substitution into In_{11}^{7-} is interesting relative to other examples. Extended Hückel calculations on the parent give (within the Mulliken approximation) charges of −0.31, −0.54 and −0.83 on the capping (In1), axial (In2) and prismatic (In3) sites. Thus, the electron-poorer (and also heavier) mercury substitutes at the most negative site – the one that also has the fewest bonding neighbors. This mode agrees on both counts with the disposition observed for the parallel substitution of thallium within the clusters $TlSn_9^{3-}$ (axial Tl in a bicapped square antiprism) and $TlSn_8^{3-}$ (capping in a tricapped trigonal prism) that have been isolated from nonaqueous solutions as salts with largely organic cations [11]. These dispositions contradict the usual wisdom in, *e.g.* carboranes, where the electron-richer heteroatom carbon substitutes at the more negative sites. However, these contrary examples also involve substantial differences in bond strength and character, and orbital size. It is also interesting to note that the clusters In_{11}^{7-} and $In_{10}Hg^{8-}$ as well as the centered members $In_{10}Zn^{8-}$ (D_{4d}) and $In_{10}Ni^{10-}$ ($\sim C_{3v}$) are all isoelectronic in s and p electrons, yet the stable eleven-atom polyhedra for these involve three different examples, one homoatomic, one substitutional and two interstitial. The

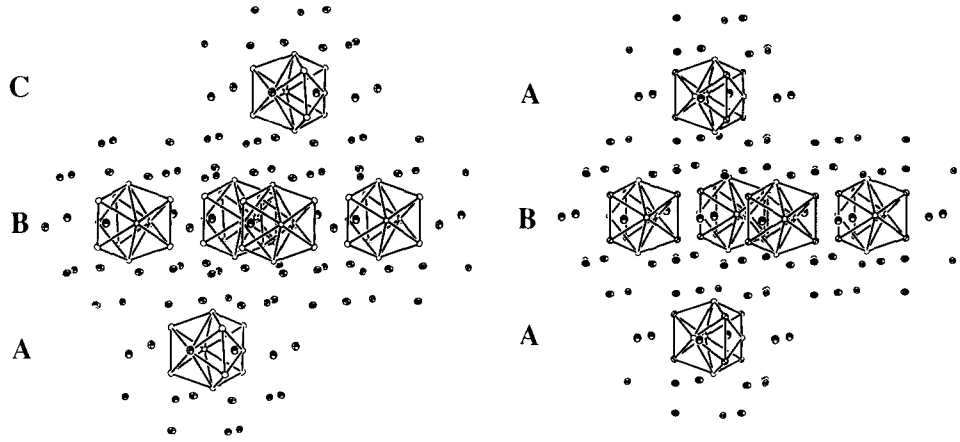

Fig. 2. The close-packed layering of clusters and potassium ions in (left) K_8In_{11} ($R\bar{3}c$) and (right) $K_8In_{10}Hg$ ($P6_3/m$) ($\vec{c}$ vertical).

configurations that these systems have to choose from appear to be substantial in number, with energy differences and structural preferences that appear to be small and subtle, respectively.

Extended Hückel MO calculations performed earlier on In_{11} showed that a cluster with this geometry is hypoelectronic and requires $2n-4=18$ p-electrons for skeletal bonding, *i.e.* In_{11}^{7-}. The eighth electron in K_8In_{11} was presumed to be delocalized, possibly within the double K1 layers, making the compound metallic. Some properties were consistent, a temperature-independent $\chi_M(\text{corr}) = +(1-2)\times10^{-4}$ emu mol^{-1} and $\rho_{295} \sim 600$ $\mu\Omega$ cm with a positive temperature coefficient [1]. The complete reduction of the anion by all eight potassium valence electrons in $K_8In_{10}Hg$ leads to the isoelectronic $In_{10}Hg^{8-}$ species with a closed shell of skeletal electrons. The substitution of one and only one mercury atom in the same cluster is strong support for our earlier analysis of K_8In_{11}.

The measured magnetic susceptibilities of $K_8In_{10}Hg$ were again corrected for diamagnetism from the ion cores (-3.3×10^{-4} emu mol^{-1}) and for the Larmor precession of the nine electron pairs in the skeletal orbitals of the cluster (-3.0×10^{-4} emu mol^{-1}). The net result is plotted on Fig. 3 together with comparable data for K_8In_{11}, the two data sets having received the same corrections save for the small difference of the mercury core. Considerable electron pairing is evident between the Pauli paramagnetic K_8In_{11} and the diamagnetic $K_8In_{10}Hg$ where a Zintl (valence) phase would be expected. (The tails at low temperature are common features usually attributed to small amounts of para- or ferromagnetic impurities). No superconductivity was seen for $K_8In_{10}Hg$ (or the phases containing centered indium clusters) at fields of 50–100 Oe over the range 2–10 K. The diamagnetic properties of $K_8In_{10}Hg$, $K_8In_{10}Zn$ and $K_{10}In_{10}Ni$ are virtually superimposable [12].

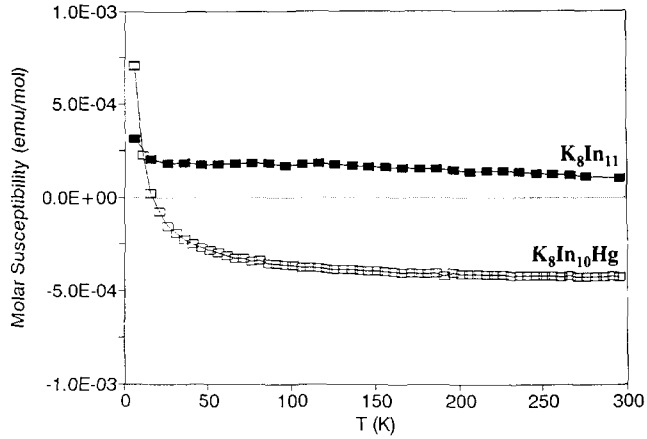

Fig. 3. Molar magnetic susceptibility *vs.* T for K_8In_{11} and $K_8In_{10}Hg$. Both data sets have been corrected for core diamagnetism and with the same orbital (Lamour) precession contribution from the cluster–bonding electron pairs.

In contrast, $K_8In_{10}Hg$ was found to have an electrical resistivity of $\rho_{295} \sim 270$ $\mu\Omega$ cm with a coefficient of $+0.48\%$ per degree. While the absolute value for ρ may be uncertain by a factor of about three, the coefficient should be fairly reliable. Such properties, *i.e.* strong diamagnetism and conductivities of a poor metal or a semimetal, have also been observed for another salt that is surmised to have a closed-shell polyanion, $K_8In_{10}Zn$ [4]. (Two probe data indicate that $K_{10}In_{10}Ni$ is a very poor conductor [12], as is the $^2_\infty[In_6^{4-}]$network in Rb_2In_3 [13]). A metal like indium in negative oxidation states will, of course, have elevated valence energies, conceivably enough to afford some overlap of valence and conduction bands. The magnetic and conduction properties of $K_8In_{10}Hg$ are probably best attributed to a semimetallic behavior. In any case, the results should not obliterate the clear importance of covalent In–In bonding below some high-lying conduction in what could be a "metallic Zintl phase" [14].

Finally, we note that the magnitudes of both the observed diamagnetism and the electronic conduction may be exaggerated via the same effects that influence many heavy main-group metals themselves. Indium is both diamagnetic ($\chi_{293}(\text{corr}) = -45 \times 10^{-6}$ emu mol^{-1}) and metallic ($\rho_{293} = 8.4$ $\mu\Omega$ cm [15]). Large orbital overlaps and low densities of states at E_F classically go hand-in-hand with small effective electron masses. This in turn affords smaller Pauli-paramagnetic but larger diamagnetic Landau contributions for the conduction electrons as well as high charge mobilities and thence enhanced conductivity [16].

Acknowledgments

The use of the "Q" apparatus was provided by J. Shinar. This research was supported by the US Department of Energy, Office of Basic Energy Sciences, Materials Sciences Division. The Ames Laboratory is operated for the DOE by Iowa State University under contract No. W-7405-Eng-82.

References

1 S.C. Sevov and J.D. Corbett, *Inorg. Chem., 30* (1991) 4875.
2 S.C. Sevov and J.D. Corbett, *Inorg. Chem., 31* (1992) 1895.
3 S.C. Sevov and J.D. Corbett, *J. Solid State Chem., 103* (1993) 114.
4 S.C. Sevov and J.D. Corbett, *Inorg. Chem., 32* (1993) 1059.
5 J.D. Corbett and S.C. Sevov, *Z. Phys.D.–Atoms, Molecules and Clusters, 26* (1993) in press.
6 S.C. Sevov and J.D. Corbett, unpublished research.
7 C. Belin and M. Tillard-Charbonnel, *Prog. Solid State Chem., 22* (1993) 59.
8 K. Wade, *Adv. Inorg. Chem., Radiochem., 18* (1976) 1.
9 G.M. Sheldrick, SHELXS-86; Universität Göttingen, 1986.
10 J. Shinar, B. Dehner, B.J. Beaudry and D.T. Peterson, *Phys. Rev., 37B* (1988) 2066.
11 R.C. Burns and J.D. Corbett, *J. Am. Chem. Soc., 104* (1982) 2804.
12 S.C. Sevov and J.D. Corbett, *J. Am. Chem. Soc., 115* (1993) in press.
13 S.C. Sevov and J.D. Corbett, *Z. Anorg. Allg. Chem., 619* (1993) 128.
14 R. Nesper, *Prog. Solid State Chem., 20* (1990) 1.
15 *CRC Handbook of Chemistry and Physics*, CRC Press, Boca Raton, FL, 65th edn., 1984, E-108, F-120.
16 C. Kittel, *Introduction to Solid State Physics*, J. Wiley, New York, 2nd edn., 1956, p. 293.